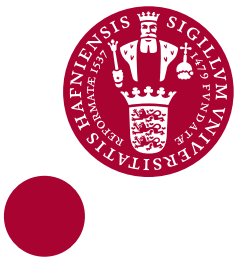

Utility of (11)C-methionine and (11)C-donepezil for imaging of Staphylococcus aureus induced osteomyelitis in a juvenile porcine model

comparison to autologous (111)In-labelled leukocytes, (99m) Tc-DPD, and (18)F-FDG

Afzelius, Pia; Alstrup, Aage Ko; Schønheyder, Henrik C; Borghammer, Per; Jensen, Svend B; Bender, Dirk; Nielsen, Ole L

Published in:
American Journal of Nuclear Medicine and Molecular Imaging

Publication date:
2016

Document version
Publisher's PDF, also known as Version of record

Am J Nucl Med Mol Imaging 2016;6(6):286-300
www.ajnmmi.us /ISSN:2160-8407/ajnmmi0035340

Original Article

Utility of ^{11}C-methionine and ^{11}C-donepezil for imaging of *Staphylococcus aureus* induced osteomyelitis in a juvenile porcine model: comparison to autologous ^{111}In-labelled leukocytes, ^{99m}Tc-DPD, and ^{18}F-FDG

Pia Afzelius[1], Aage KO Alstrup[2], Henrik C Schønheyder[3,4], Per Borghammer[2], Svend B Jensen[5,6], Dirk Bender[2], Ole L Nielsen[7]

[1]Department of Diagnostic Imaging, North Zealand Hospital, Hillerød, University Hospital of Copenhagen, Copenhagen, Denmark; [2]Department of Nuclear Medicine and PET Centre, Aarhus University Hospital, Aarhus, Denmark; [3]Department of Clinical Microbiology, Aalborg University Hospital, Aalborg, Denmark; [4]Department of Clinical Medicine, Aalborg University, Aalborg, Denmark; [5]Department of Nuclear Medicine, Aalborg University Hospital, Aalborg, Denmark; [6]Department of Chemistry and Biochemistry, Aalborg University, Aalborg, Denmark; [7]Department of Veterinary Disease Biology, University of Copenhagen, Copenhagen, Denmark

Received August 19, 2016; Accepted August 31, 2016; Epub November 30, 2016; Published December 15, 2016

Abstract: The aim of this study was to compare ^{11}C-methionine and ^{11}C-donepezil positron emission tomography (PET) with ^{111}In-labeled leukocyte and ^{99m}Tc-DPD (Tc-99m 3,3-diphosphono-1,2-propanedicarboxylic acid) single-photon emission computed tomography (SPECT), and ^{18}F-fluorodeoxyglucose (^{18}F-FDG) PET to improve detection of osteomyelitis. The tracers' diagnostic utility where tested in a juvenile porcine hematogenously induced osteomyelitis model comparable to osteomyelitis in children. Five 8-9 weeks old female domestic pigs were scanned seven days after intra-arterial inoculation in the right femoral artery with a porcine strain of *Staphylococcus aureus.* The sequential scan protocol included Computed Tomography, ^{11}C-methionine and ^{11}C-donepezil PET, ^{99m}Tc-DPD and ^{111}In-labelled leukocytes scintigraphy, and ^{18}F-FDG PET. This was followed by necropsy of the pigs and gross pathology, histopathology, and microbial examination. The pigs developed a total of 24 osteomyelitic lesions, 4 lesions characterized as contiguous abscesses and pulmonary abscesses (in two pigs). By comparing the 24 osteomyelitic lesions, ^{18}F-FDG accumulated in 100%, ^{111}In-leukocytes in 79%, ^{11}C-methionine in 79%, ^{11}C-donepezil in 58%, and ^{99m}Tc-DPD in none. Overall, ^{18}F-FDG PET was superior to ^{111}In-leukocyte SPECT and ^{11}C-methionine in marking infectious lesions.

Keywords: ^{11}C-methionine, ^{11}C-donepezil, ^{111}In-labelled leukocytes, ^{99m}Tc-DPD, ^{18}F-FDG, *Staphylococcus aureus,* osteomyelitis, porcine, swine, pig, PET/CT, scintigraphy, SPECT/CT, CT

Introduction

Bone infections in children result primarily from hematogenous seeding of bacteria in long bones in the lower extremities [1], and *Staphylococcus aureus* (*S. aureus*) is by far the most frequent contributing agent. Juvenile hematogenous osteomyelitis (HO) has an incidence of 2-13/100,000 in high-income countries [2-4] but is more frequent in low-income countries affecting approximately 1.5% of all children [5-10]. It is particularly common between 2-12 years of age and is more common in boys (Boy:Girl of 3:1) [11]. Approximately 50% of cases occur in preschool children. Younger children primarily experience acute HO due to the rich vascular supply in their growing bones. Circulating microorganisms tend to start the infection in the metaphyseal ends of the long bones due to seeding of septic emboli aided by the slow circulation in the capillary loops in the metaphyseal growth zone. The presence of vascular connections between the metaphysis and the epiphysis, the transphyseal blood vessels, makes infants particularly susceptible to epiphyseal spread and arthritis of the adjacent joint. HO is always a serious disease because of a tendency to become chronic or recurrent. Early diagnosis and initiation of therapy is essential to prevent disease progre-

ssion and to reduce potentially serious complications. Conventional radiography on hospital admission cannot rule out acute osteomyelitis. Osteomyelitic foci must extend at least 1 cm and lead to a 30-50% reduction of bone mineral content to produce noticeable radiographic changes [12]. Early findings may be subtle, and changes may not be obvious within the first 5-7 days in children and 10-14 days in adults. Magnetic resonance imaging (MRI), bone scintigraphy, and computed tomography (CT) are central imaging modalities for diagnosing acute osteomyelitis in children [13], the latter two, however, adding substantially to the radiation exposure of the child. MRI is often considered the best imaging method but is not always available and requires anesthesia in young children. Bone scintigraphy demonstrates osteoblastic activity and is considered highly sensitive but not particularly specific. ^{18}F-fluordeoxyglucose (FDG) positron emission tomography (PET) may have the highest diagnostic accuracy for confirming or excluding chronic osteomyelitis in comparison with bone scintigraphy, MRI, and leukocyte scintigraphy. However, most studies have addressed ^{18}F-FDG PET for use in the axial skeleton [14, 15] and not in the appendicular skeleton. Highly sensitive inflammation and infection specific tracers especially for PET imaging are much needed and the focus of several research projects. When using imaging modalities in children, the balance between radiation exposure and faster diagnostics could favor the latter, depending on the individual case.

In search for superior inflammation/infection tracers, we have previously compared ^{111}In-leukocytes, ^{18}F-FDG and ^{11}C-methionine in a porcine model of *S. aureus* osteomyelitis 7 days after inoculation [16]. The study included 5 osteomyelitis lesions. Based on this rather limited number of lesions, we concluded that ^{18}F-FDG was superior to ^{111}In-leukocytes to identify bone lesions; however, the labeled leukocyte SPECT was performed as early scans only 6 h after injection. ^{11}C-methionine was the least successful among the three tracers to identify osteomyelitis, but did accumulate in soft tissue lesions. By increasing the injection to scan time interval to the more traditional 24 h we aim to demonstrate that this protocol is comparable to the 6 h labeled leukocyte protocol, but inferior to ^{18}F-FDG PET. Furthermore, by increasing the activity of ^{11}C-methionine, we aim to demonstrate that this tracer can be used as an alternative to ^{18}F-FDG in early osteomyelitis. As a consequence of the so called "cholinergic anti-inflammatory pathway" mediated by acetylcholine, acetylcholine esterase activity should be upregulated in inflammatory tissue [17]. Thus, we hypothesized that the C-11-labeled acetylcholine esterase inhibitor donepezil might serve as a marker of osteomyelitis. Finally, we aimed to reveal the utility of bone scintigraphy in juvenile pigs with osteomyelitis.

Materials and methods

Pigs and the S. aureus model

Five pigs (A-E), all clinically healthy, specific pathogen-free Danish landrace-Yorkshire cross-breed female pigs aged 8-9 weeks, were purchased from a local commercial pig farmer. After one week of acclimatization the pigs were, under anesthesia, inoculated with a suspension of a porcine strain of *S. aureus* (S54F9) (10^5 colony forming units per kg in 1.0 to 1.5 mL) into the femoral artery of the right hind limb, to induce osteomyelitis, as described elsewhere [16, 18-20]. After onset of clinical signs e.g. limping of the right hind limb, which occurred in all pigs, the pigs were once supplied with a single intramuscular (IM) procaine benzylpenicillin 10,000 IE/kg (Penovet, Boehringer Ingelheim, Copenhagen, Denmark) injection. Buprenorphine (45 μg/kg Temgesic (Reckitt Benckiser, Berkshire, England)) were given three times daily from time of inoculation until euthanasia [21]. One week after inoculation the pigs had obtained a body weight of 21-23.5 kg (**Table 1**). The pigs were then scanned and finally euthanized with an overdose of pentobarbitale (100 mg/kg IV).

We have previously reported that some pigs in this osteomyelitis model will develop hematogenous dissemination of *S. aureus* leading to e.g. embolic pneumonia [16, 19]. In order to reduce the frequency of these additional lesions we used animals aged 8-9 weeks and administered procain benzylpenicillin intramuscularly as described by Alstrup et al. [20]; these measures also aimed to reduce suffering of the pigs. On signs of anorexia for more than 24 hours, shallow respiration, or fever decision of euthanasia was taken by a veterinarian. The study was approved by the Danish Animal Experimentation Board (no. 2012-15-2934-000123). All facilities were approved by the Danish Occupational Health Surveillance.

Table 1. Body weight of pigs, sequence of tracer injection, tracer activity, and time points of diagnostic scans

Pigs	Tracer sequence	Time points, injection	Time points, diagnostic scan	Injected activity (MBq) and labeling percent
A, body weight 22 kg				
	^{11}C-methionine	10:18	11:21	516
	^{11}C-donepezil	12:04	13:09	491
	^{99m}Tc-DPD	14:08	16:20	180-200
	^{111}In-leukocytes	17:00 previous day	16:35	20.8; 69.7%[a]
	^{18}F-FDG	23:40	00:46 following day	415
B, body weight 23 kg				
	^{11}C-methionine	10:05	11:11	537
	^{11}C-donepezil	12:04	13:08	472
	^{99m}Tc-DPD	13:45	15:45	180-200
	^{111}In-leukocytes	16:25 previous day	16:28	15.7; 57.7%[a]
	^{18}F-FDG	21:07	22:14	398
C, body weight 21 kg				
	^{11}C-methionine	10:52	12:00	363
	^{11}C-donepezil	12:55	14:17	525
	^{99m}Tc-DPD[b]	14:48	16:55	180-200
	^{111}In-leukocytes[b]	16:26 previous day	17:04	24.4; 74.6%[a]
	^{18}F-FDG[b]	NT	NT	NT
D, body weight 23 kg				
	^{11}C-methionine	10:40	11:46	530
	^{11}C-donepezil	12:46	13:50	486
	^{99m}Tc-DPD	14:20	17:00	198
	^{111}In-leukocytes	17:05 previous day	17:15	19.3; 62.5%[a]
	^{18}F-FDG	23:46	00:52 following day	393
E, body weight 23.5 kg				
	^{11}C-methionine	11:19	12:27	551
	^{11}C-donepezil	13:16	14:20	520
	^{99m}Tc-DPD	14:50	17:54	197
	^{111}In-leukocytes	17:00 previous day	18:11	18.8; 67.0%[a]
	^{18}F-FDG	00:21 following day	01:26 following day	497

a: Labeling efficacy. b: Pig died 15:20; thus ^{99m}Tc-DPD and ^{111}In-leukocyte SPECT were performed on a dead pig and ^{18}F-FDG PET was not performed.

Blood glucose and serum C-reactive protein

Blood glucose was measured using a Radiometer ABL (Radiometer, Brønshøj, Denmark) or a fast-test system for diabetic patients. Serum C-reactive protein (CRP) measurements were performed according to Heegaard et al. [22].

Preparation of tracers

^{11}C and ^{18}F were produced at the PET Centre Aarhus University Hospital using either a PETtrace 800 series cyclotron (GE Healthcare, Uppsala, Sweden) or a Cyclone 18/18 cyclotron (IBA, Louvain La Neuve, Belgium).

^{11}C-methionine and ^{11}C donepezil were synthesized as described elsewhere [23, 24]. Briefly, ^{11}C-methionine was synthesized by [^{11}C] S-methylation of L-homocysteine thiolactone with methyl iodide [25] followed by preparative HPLC using a GE Healthcare Tracerlab FXC PRO synthesizer. L-homocysteine thiolactone was supplied by Sigma (Sigma-Aldrich Denmark, Brøndby, Denmark). Other chemicals including iodine or acetone were supplied by either Sigma-Aldrich (Sigma-Aldrich A/S, Brøndby, Denmark) or Aarhus University Hospital Pharmacy (Aarhus, Denmark). The radiochemical purity exceeded 95% and the specific radioac-

tivity generally was higher than 37 GBq/μmol at end of production. 363-551 MBq of ^{11}C-methionine was injected and PET/CT was performed 63-68 min later (**Table 1**).

In brief, ^{11}C-donepezil synthesis started with the conversion of cyclotron-derived ^{11}C-carbon to ^{11}C-methyliodide, which was trapped in dimethyl sulphoxide (300 mL) containing 1 mL of 2 M NaOH and 5-O-desmethyl donepezil (0.5 mg). The mixture was heated at 80°C for 5 min; purification of ^{11}C-donepezil was performed by high-performance liquid chromatography. 5-O-desmethyl donepezil was supplied by Toronto Research Chemicals (Toronto, Canada) and all other chemicals were supplied by either Sigma-Aldrich A/S or Aarhus University Hospital Pharmacy (Aarhus, Denmark). The chemical purity exceeded 99.9%. Specific radioactivity generally exceeded 40 GBq/μmol at time of injection. 472-525 MBq ^{11}C-donepezil was injected and PET/CT was performed after 64-82 min (**Table 1**).

^{111}In-labeled leukocytes may not be recommended in children due to the effective dose equivalent being about three times as high in children (5 years old) as in adults [26], but are occasionally used in order to perform the dual isotope technique using different energy windows to detect ^{99m}Tc and ^{111}In simultaneously. We chose ^{111}In for this reason also to carry out both bone and leukocyte scintigraphy within a tight time schedule. ^{111}In-labeled leukocytes were prepared according to the instructions given by the producer. The ^{111}In oxine was obtained from Mallinckrodt, Pharmaceutical, Copenhagen, Denmark. The ^{111}In-labelling of leukocytes included isolation of the leukocyte fraction from autologous full blood using sedimentation and centrifugation [27]. Labeling of the leukocyte preparations and reinjection were performed on day 6 post inoculation (PI), i.e. one day in advance of the SPECT and PET scans (day 7 PI). Injected activity of ^{111}In-labeled leukocytes was 15.7-24.4 MBq and imaging was performed about 23 h-25 h after injection (**Table 1**). Scintigrams were complemented by regional SPECT/CT of pelvis and hind limbs.

^{99m}Tc-DPD was prepared according to the instructions given by the manufacturer (Mallinkrodt Pharmaceuticals). The bone scintigraphies were performed 120-160 min after intravenous injection of 180 to 200 MBq ^{99m}Tc-labeled methylene diphosphonate thus using a medium energy collimator. Normal activity for children is 9.3 MBq per kg (**Table 1**).

^{18}F-FDG was produced by a standard procedure applying a GE Healthcare MX Tracerlab synthesizer, Mx cassettes supplied by Rotem Industries (Arava, Israel) and chemical kits supplied by ABX GmbH (Radeberg, Germany). The radiochemical purity was higher than 99%. Normal recommended activity in children is 3.7-5.2 MBq per kg [15]. Pigs were given 17.1-21.1 MBq/kg, and scanning performed 64-67 min after injection (**Table 1**).

PET, CT, scintigraphy, and SPECT

All examinations at the PET Center Aarhus University Hospital were performed with an integrated PET/Computed tomography (CT) system (Siemens Biograph True point 64 PET/CT, Siemens, Erlangen, Germany), one bed position spanning 21 cm. The pigs were anaesthetized with propofol, intubated (for mechanical ventilation) and placed in dorsal recumbence as described by Alstrup and Winterdahl [28]. Initially a scout view was obtained to secure body coverage from snout to tail. A CT scan for attenuation correction of PET data was obtained first. PET images were reconstructed using the iterative TrueX algorithm (Siemens) and CT and PET data were co-registered for image fusion by the system.

At the Nuclear Medicine Department, Aalborg University Hospital pigs were placed in a dorsal recumbent position and PET/CT scanned applying an integrated system (GE VCT Discovery True 64 PET/CT 2006, GE Healthcare, USA), one bed position spanning 15 cm. PET images were reconstructed using an iterative algorithm (ViewPoint algorithm (GE Healthcare)) and attenuation correction based on low-dose CT.

Planar gamma imaging supplied with single photon emission computed tomography (SPECT)/CT was performed in Aalborg on the pelvic limbs and region included in a single bed position using a Symbia T16 SPECT/CT (Siemens Medical Solutions, Hoffman Estates, Illinois, USA). The residual activity from PET isotopes was recognized as a source of background radiation on the SPECT scanner, and we therefore applied the medium-energy collimators as suggested in [29]. Whole-body planar images were acquired on a dual-headed

gamma camera with simultaneous anterior and posterior whole-body acquisition.

All PET scans were first performed as dynamic PET of the pelvic and hind limb region followed by a later static whole body scan of 5 min (PET Centre Aarhus) and 6 or 12 min (Dept. of Nuclear Medicine Aalborg) duration per bed position.

Tracers were injected into a surgical placed catheter in the jugular vein. The tracers applied, their activity, and their sequence in the individual pigs (pigs A-E) are presented in **Table 1**. The minimum time span from the first injection to last scan was 6 h 12 min (pig C that died); the maximum time span was 14 h 56 min (pig A).

Arterial blood samples were collected from a surgically placed catheter in a carotid artery and tested for intact PET tracer content in order to determine input function and to allow kinetic modeling. However, the results of the dynamic PET scans, ^{15}O-water scan, and kinetic modeling will be reported elsewhere, as will the results of the ^{68}Ga-Siglec-9 scan.

Reading the scans

PET with ^{11}C-Methionine, ^{11}C-donepezil, and ^{18}F-FDG, as well as scintigraphy and SPECT with ^{99m}Tc-DPD and ^{111}In-leukocytes and CT were read individually. PET and scintigraphy were also read as fused images with CT. All scans were evaluated by an experienced specialist in nuclear medicine and CT.

Gross pathology, histopathology, and microbiology

Following euthanasia, the carcass was kept at 4°C for 8 hrs, transported for another 4 hrs at room temperature, and necropsied as described earlier [30]. During necropsy, predefined biopsies or swabs for microbial cultivation were obtained from the bone marrow, lungs, brain, liver, spleen, and kidney. Predefined tissues and organs were sampled for histopathology, including bone samples from the right pelvic limb and the lungs. Identification of gross lesions at necropsy resulted in additional sampling for histopathology and microbiology. On average 13 specimens were obtained for culture per autopsy. The full set of results will be presented elsewhere. Here we report macroscopic and CT findings, histopathology including immunohistochemistry for *S. aureus*, and microbiology findings sufficient to secure the final diagnosis.

Histopathology (hematoxylin and eosin stain) and immunohistochemistry for *S. aureus* was performed as previously described [19]. For microbiology, biopsy material and swabs were inoculated on 5% horse blood agar (SSI Diagnostica, Hillerød, Denmark) and inoculated at 35°C in ambient atmosphere for 24 hours. *S. aureus* was confirmed by Gram stain and a positive commercial clumping factor test. A full antibiogram was performed to distinguish the pan-susceptible challenge strain from methicillin-resistant *S. aureus* (clonal complex 398) which is prevalent in Danish pig farms.

Results

Tracer activity, injection time, and scan time concerning pig A-E are summarized in **Table 1**. Labeling efficacies of leukocytes were 57.7-74.6%, which is about the same as expected in humans [27, 31].

Pig clinical presentation and lesions

All five pigs (A-E) were without clinical signs of disease prior to inoculation. Serum C-reactive protein (CRP) content was 2-7 mg/L, normal ranges (0-15 mg/L) in pig A-D. The CRP in pig E was 109 mg/L prior to inoculation, but no cause was found for this elevation. The pig had prior to inoculation a normal leukocyte count, normal neutrophile count, no clinical signs of disease, no tail or ear bite lesions, and no skin wounds in other locations; and a normal pulse rate and oxygen-saturation. At necropsy, no lesions besides those associated with inoculation with the well characterized *S. aureus* strain were observed. We have retrospectively contacted the laboratory where this CRP was analyzed, and we have been informed that the serum sample could have been desiccated at the time of analysis and the result thus not reliable. All pigs developed clinical signs of infection after inoculation. CRP increased in all pigs, also in the pig E to reach a level ranging from 23 to 218 mg/L (pig E 155 mg/L). On day 7 the pigs had body temperature peaks of 37.2-41.7°C. Pig C that died had a normal core temperature and the lowest heart rate of the 5 pigs. Highest heart rates during the examination period ranged from 88 to 136 beats per min. The oxygen saturation was mostly between 99 and 100%.

Table 2. Lesions defined by gross pathology, histopathology and/or CT in 5 juvenile pigs with hematogenous *S. aureus* osteomyelitis induced by right femoral artery inoculation. *S. aureus* culture results after necropsy is summarized in the lower row

Pig lesion	A	B	C	D	E	Total
Osteomyelitis[A]	3	5	6	4	6	24
Sequestration	3	5	4	4	6	22
Osteolysis adjacent cortical bone	1	3	4	3	6	17
Contiguous periosseous abscess	0	0	1	1	2	4
Arthritis	0	0	0	0	1	1
Hematoma/abscess at inoculation site	0	1	0	0	1	2
Lymph node enlargement	2	1	2	1	2	8
S. aureus culture confirmed after necropsy	NT[B]	Femur biopsy	Tibia biopsy and periosseous abscess	Femur biopsy and periosseus abscess hock	Periosseus abscess 4th digit	

A: Location of the lesions in right hind limb is presented in **Figure 1**. B: NT: not tested. Immunohistochemical staining for *S. aureus* was performed on femur instead (see **Figure 1**).

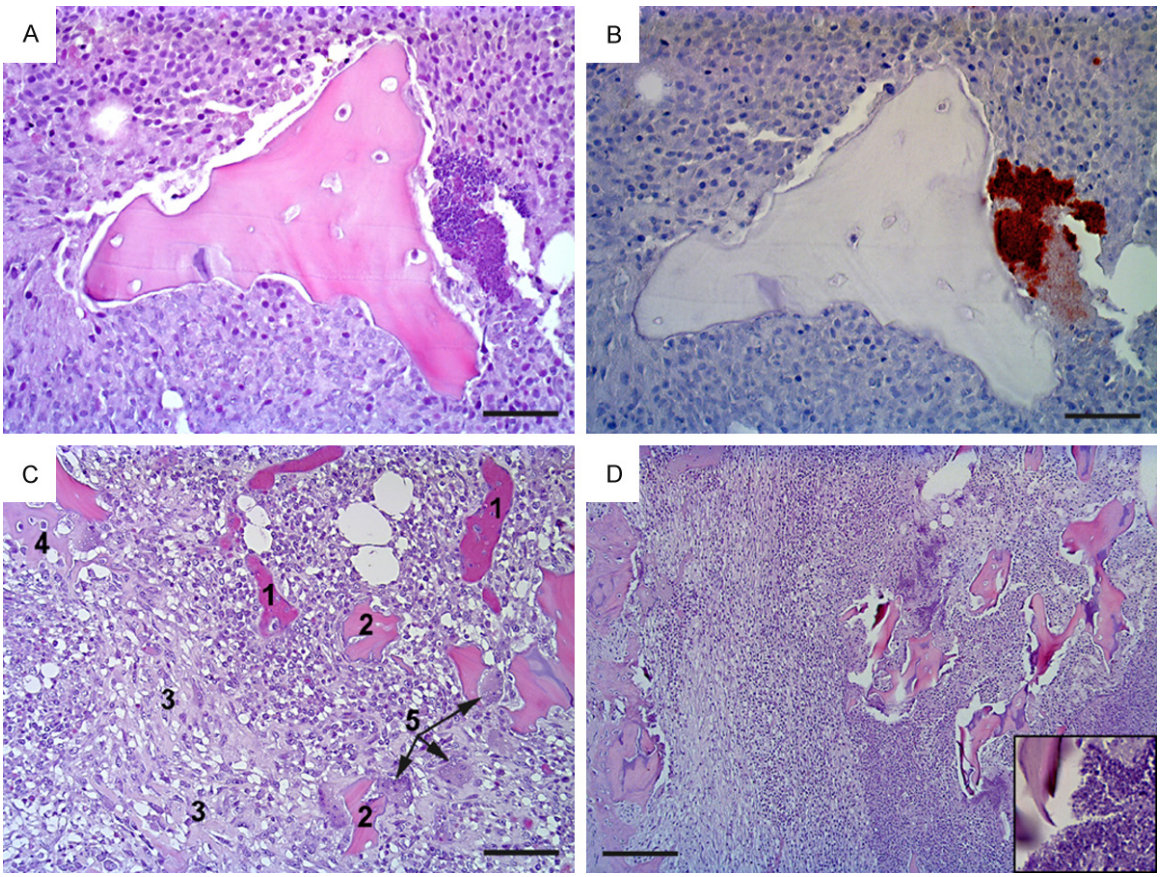

Figure 1. Histopathology of osteomyelitis in pig A (pictures A-C) and pig E (picture D). Pig A: (A) shows the center of a bone lesion with necrotic trabecular bone surrounded by necrotic neutrophils (hematoxylin and eosin stain); at the right hand side of the figure is a colony of bacteria (blue) which in (B) are identified as *S. aureus* (brown) (immunohistochemistry); (C) shows the periphery of the lesion, disclosing blood vessels packed with erythrocytes (1), necrotic bone (2), fibroplasia (3), new bone formation (4) and osteoclasts (5) (hematoxylin and eosin). Pig E: (D) presents a similar lesion to that in in pig A, i.e. a subacute, suppurative, and necrotizing osteomyelitis, here bordering the cortex of the bone (left hand side) (hematocylin and eosin); insert is a close up of the bacteria seen in the necrotic center. Bar (A and B) = 25 μm, (C) = 50 μm, and (D) = 100 μm.

Table 2 displays the *S. aureus* lesions diagnosed by gross pathology, histopathology, and/or CT and/or microbial cultivation for each of the pigs. Evaluation of hematoxylin and eosin stained sections of bone lesions from pig A and E identified subacute, suppurative, and necro-

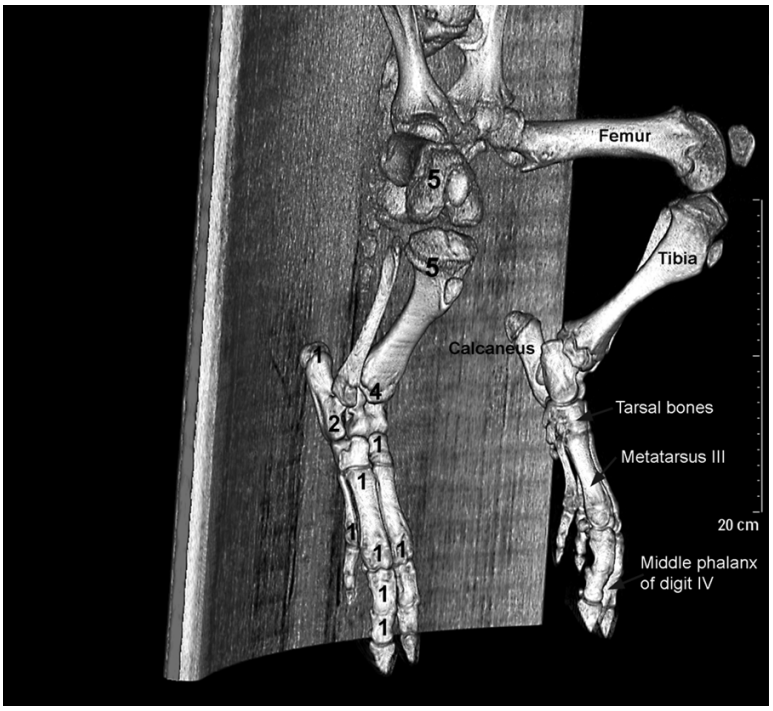

Figure 2. 3D skeleton generated from CT-scan of a healthy juvenile pig. Pelvis and hind limbs are shown. Numbers of osteomyelitic lesions are shown in individual bones and femur, tibia, tarsal bones, metatarsus III, and middle phalanx of digit IV are indicated.

tizing osteomyelitis with extensive osteomyelitis (**Figure 1**). No microbial cultivation was performed in pig A. Instead, positive identification of *S. aureus* was performed in one of the lesions by immunohistochemistry (**Figure 1B**). A total number of 24 osteomyelitic lesions were found close to the metaphyses in long bones 7 days after inoculation with *S. aureus*. Two pigs had embolic seeding in the lungs. Data are not shown.

Figure 2 shows the anatomical localization of the osteomyelitic lesions 7 days after inoculation with *S. aureus*. Typical locations after injection into the right femoral artery were distal femur and proximal and distal tibia covering 61% of lesions in hind limb. Locations were more variable in the smaller and more peripheral bones. In one of the pigs, we also saw a lesion in the right humerus (not shown in the figure).

Performance of the tracers ^{11}C-methionine, ^{11}C-donepezil, ^{111}In-leukocytes, ^{99m}Tc-DPD, and ^{18}F-FDG

^{11}C-methionine lesion to background activity was improved in this study using higher activity (**Figures 3**, **4B**) compared to our previous study [19] and so was the ability to detect osteomyelitic lesions. Methionine seems to accumulate in the profound part of the lesions.

Table 3 summarizes the performance of the different tracers. ^{18}F-FDG detected 18/18 osteomyelitic foci (100%), ^{11}C-methionine 19/24 (79%), ^{111}In-leukocytes 19/24 (79%), ^{11}C-donepezil 14/24 (58%), and ^{99m}Tc-DPD 0/24 (0%).

A representative example of accumulation and performance of the different tracers in an osteomyelitic lesion of medial distal femur condyle is presented in **Figure 4**. ^{11}C-methionine PET is shown in **Figure 4B** and ^{11}C-donepezil PET is shown in **Figure 4C**. The corresponding CT scan is shown in **Figure 4A**. ^{99m}Tc-DPD scintigraphy is shown in **Figure 4E** and ^{111}In-leukocyte scintigraphy is shown in **Figure 4F**. The corresponding CT is shown in **Figure 4D**. Finally, ^{18}F-FDG PET is shown in **Figure 4H** with the corresponding CT shown in **Figure 4G**. The SUV color-scale is the same in all PET-pictures, showing that ^{18}F-FDG (**Figure 4H**) and ^{11}C-methionine (**Figure 4B**) had higher accumulation of activity than ^{11}C-donepezil (**Figure 4C**).

^{11}C-methionine accumulated in all enlarged probably reactive regional lymph nodes, i.e. 8/8, whereas ^{11}C-donepezil accumulated in 6/8, ^{18}F-FDG accumulated in 3/6 detected, and ^{111}In-labled leukocytes accumulated in 3/8. All tracers accumulated in all the contiguous periosseous and inoculation related abscesses.

^{111}In-leukocyte distribution in anterior and posterior projections 24 h after inoculation in an adult human without demonstrable infection is compared to the distribution of ^{111}In-leukocytes in ventral and dorsal projection in a juvenile pig also without infection (**Figure 5**). Activity was seen in lungs, spleen and liver of the pig. The area without activity in the upper abdomen represents a full stomach. There is only a very short transient hold-up in normal lungs in

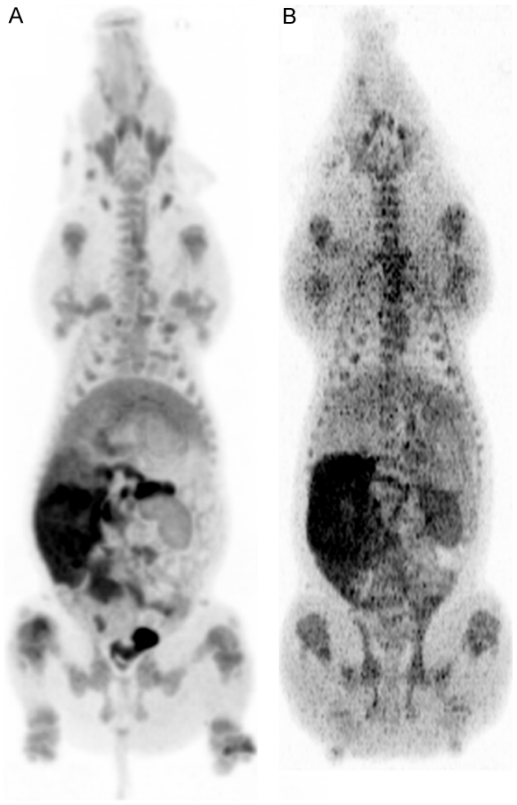

Figure 3. MIP (Maximum Intensity Projections)s of two juvenile pigs ventral views showing bio distributions of ^{11}C-methionine and back ground activity on PETs. A: High ^{11}C-methionine activity injected. B: Low ^{11}C-methionine activity injected [19].

humans [27]. In juvenile pigs the lungs, however, serve as a retriculoendothelial organ housing many intravascular macrophages, and the pig had scintigraphy performed 6 h after inoculation of ^{111}In-leukocytes [19].

Distribution of ^{99m}Tc-DPD in a juvenile pig was comparable to distribution in a seven years old child (**Figure 6**). Note the accumulation in growth zones in both species, and absence of accumulation in lesions in the pig (**Figure 6**, and **Figure 4E**). There were no photopenic areas on bone scintigraphy of any of the five examined pigs (A-E).

Discussion

The diagnosis of an inflammatory/infective process often relies on the visualization of anatomical changes of the affected organs. This may be highly dependent on the nature of the ongoing pathological process. Imaging techniques combining anatomical with functional data are helpful in order to describe and characterize site, extent and activity of the disease as it takes place.

Conventional radiology and CT are able to evaluate anatomical structural changes as a consequence of inflammation. The modalities show poor accuracy for the detection of early infection, when anatomical structures have not yet been affected or are only slightly affected. The accuracy may also be poor in immune incompetent patients whose inflammatory and repair mechanisms have faded. Dose reduction in pediatric imaging has been an issue for almost two decades due to the increased use of CT and the relative high effective radiation dose per examination. This is another reason for searching for and evaluating new tracers with the aim of understanding what they detect.

The different lesions seen in the pigs correspond to the model-associated lesions that were previously recorded [16, 19]. Osteomyelitis may affect any bone, with a predilection for the tubular bones of the arms and legs [13]. We found that 61% of the lesions in the hind limb were located in femoral and tibial bones (**Figure 2**) which also are common favored locations in children [13].

We have no other explanation for the elevated CRP prior to inoculation of *S. aureus* in pig E than a possible not reliable serum sample as stated by the laboratory. We did not record any clinical signs of infections prior to inoculation with *S. aureus*, and all recorded lesions were as stated above, associated with the inoculated staphylococci.

By comparing the performance of the different tracers (**Table 3** and **Figure 4**), ^{18}F-FDG performed best for detecting osteomyelitic lesions (**Figure 4H**), followed by ^{111}In-leukocytes (**Figure 4F**), ^{11}C-methionine (**Figure 4B**), and then ^{11}C-donepezil (**Figure 4C**). ^{99m}Tc-DPD did not accumulate in any osteomyelitic lesions at all (**Figure 4E**).

^{99m}Tc-DPD, an indicator of osteoblast activity could not visualize osteomyelitis in juvenile pigs (**Figures 4E**, **6B**, and **Table 3**). Normally, ^{99m}Tc-DPD will accumulate within the first week in bone lesions as seen on bone scintigraphy [32]. There have been divergent results in chil-

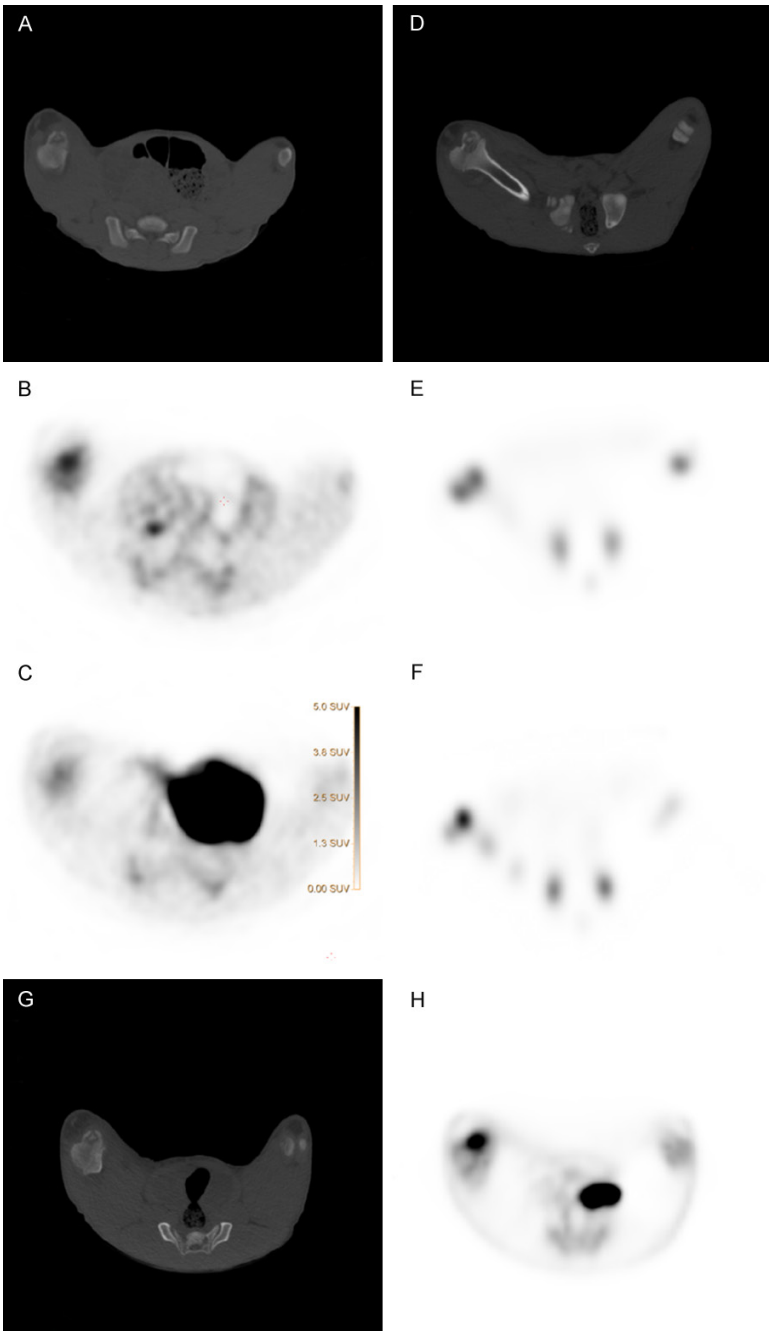

Figure 4. Osteomyelitic lesion in a medial distal femur condyle of one pig examined with CT, PET, and scintigraphies. A: CT scan and corresponding B: ^{11}C-Methionine PET/CT, and C: ^{11}C-Donepezil PET/CT. D: CT scan and corresponding E: ^{99m}Tc-DPD bone scintigraphy and F: ^{111}In-leukocyte scintigraphy, G: CT scan and corresponding H: ^{18}F-FDG-PET/CT.

dren. In the study by Riise et al. [3], bone scintigraphy had a positive predictive value of 39% and a negative predictive value of 75%. Another study has found a low sensitivity in very young children [31] but Aigner et al. have shown high sensitivity in very young children [33]. The lack of accumulation cannot be explained solely by species difference and Johansen et al. [34] have demonstrated that this model using juvenile pigs is very suitable, since it reflects the pathogenesis and pathology in children. An explanation for missing accumulation may be lack of active bone forming osteoblasts or at least a very sparse number in the lesions due to a shift towards more osteolytic activity caused by an aggressive infection/inflammation as evidenced by presence of sequestration in 22/24 lesions. Johansen et al. [35] demonstrated a drop in serum alkaline phosphatase content in this porcine model, and thus decreased bone-formation, and explained this to be an effect of osteoblasts being occupied with osteoclast activation. Histology of representative bone lesions is presented in **Figure 1** showing areas with high numbers of osteoclasts (**Figure 1C**); however a quantitative study would be needed to disclose the proportion of osteoblast to osteoclast. Pronounced lysis was evidenced in some lesions by lysis of the cortex at its thinnest points and extension of the infection into the periosteum (periostitis). Also the age of the pigs may influence the lack of ^{99m}Tc-DPD accumulation in lesions because of the tendency of bacteria to seed in the growth zones of juveniles, in the same areas where physiological accumulation normally is high (**Figure 6B**). ^{11}C-methionine accumulation was however, distinguishable in osteomylitic lesions close to or involving the growth zones.

The increased vascular permeability in inflammatory sites allows the specific migration of

Table 3. Performance of different tracers in selected lesions (indicated by number) in the pelvic and right hind limb regions in 5 juvenile pigs with hematogenous *Staphylococcus aureus* osteomyelitis induced by right femoral artery inoculation

	Tracers lesion	Total number	^{11}C-methionine	^{11}C-donepecil	^{99m}Tc-DPD	^{111}In-leukocytes	^{18}F-FDG
Pig A	Osteomyelitis	3	2	1	0	1	3
	Contiguous periosseous abscess	0	-	-	-	-	-
	Hematoma/Abscess at inoculation site	0	-	-	-	-	-
	Lymph node enlargement	0	-	-	-	-	-
Pig B	Osteomyelitis	5	5	5	0	5	5
	Contiguous periosseous abscess	0	-	-	-	-	-
	Hematoma/Abscess at inoculation site	1	1	1	0	(1)	(1)
	Lymph node enlargement	1	1	1	0	0	0
Pig C	Osteomyelitis	6	4	3	0[A]	4[A]	NT[B]
	Contiguous periosseous abscess	1	(1)	1	0[A]	(1)[A]	NT[B]
	Hematoma/Abscess at inoculation site	0	-	-	-[A]	-[A]	NT[B]
	Lymph node enlargement	2	2	1	0[A]	(1)[A]	NT[B]
Pig D	Osteomyelitis	4	4	2	0	4	4
	Contiguous periosseous abscess	1	1	(1)	0	1	1
	Hematoma/Abscess at inoculation site	0	-	-	-	-	-
	Lymph node enlargement	3	3	2	0	(1)	1
Pig E	Osteomyelitis	6	4	3	0	5	6
	Contiguous periosseous abscess	2	2	2	0	2	2
	Hematoma/Abscess at inoculation site	1	0	0	0	0	0
	Lymph node enlargement	2	2	2	0	1	2
Total	Osteomyelitis	24	19/24	14/24	0/24	19/24	18/18
	Contiguous periosseous abscess	4	4/4	4/4	0/4	4/4	3/3
	Hematoma/Abscess at inoculation site	2	0	0	0/8	0	0
	Lymph node enlargement	8	8/8	6/8	0/8	3/8	3/6

A: Scans performed on dead pig. B: NT, not tested, as the pig had died.

radiolabeled leukocytes into inflammatory foci through the cells sticking to the activated endothelium [36]. After a passive diffusion into the cells, ^{111}In-oxine dissociates and binds irreversibly to intracellular and nuclear components, without any release with time [37]. ^{111}In-labelled leukocytes lead to a high radiation dose for cells and for patients [38]. Granulocytes are not damaged by labeling, whereas lymphocytes are killed and rapidly cleared from the blood [39]. Leukocyte scintigraphy may be used in patients with vascular or orthopedic prostheses when infection is suspected [40, 41] and for the detection of bone infections [42]. The 24 h leukocyte scintigraphy did not perform better than the shorter 6 h scheduled scintigraphy we presented earlier [16], detectability was 79% (19/24) compared to 80% (4/5). Labeling efficiency is about 90% in human adult leukocytes and viability is 97% [43]. In juvenile pigs labeling efficiency was lower (58-75%). ^{111}In-oxine a lipophilic molecule enters cells by passive diffusion indicating less viable juvenile pig leukocytes. ^{111}In has a toxic effect on human adult leukocytes and may have affected juvenile pig leukocytes even more. This may occur in juvenile human leukocytes as well. The use of ^{111}In has some disadvantages: it causes a relatively high radiation burden to patients, its gamma radiation is *sub*-optimal for *in vivo* imaging, and it is not always easily available and is expensive. ^{99m}Tc is in some ways a more attractive alternative due to its shorter half-life, availability and lower cost. ^{111}In is not recommended in children but was chosen here for logistic reasons. ^{99m}Tc-labelled leukocytes may be applied in children instead due to a more favorable radiation dose. Nevertheless, because many children referred for white cell scanning have had fever for several days to weeks, and have been extensively examined by other imaging techniques In-111 labeled cells may still have a role as in chronic sepsis in general [44]. At least dosage should be decreased in pediatric patients [45]. Labeled leukocytes also have some other disadvantages: labeling is time-consuming, handling vital cells requires skilled personal, and technicians are exposed to activity during preparation procedures.

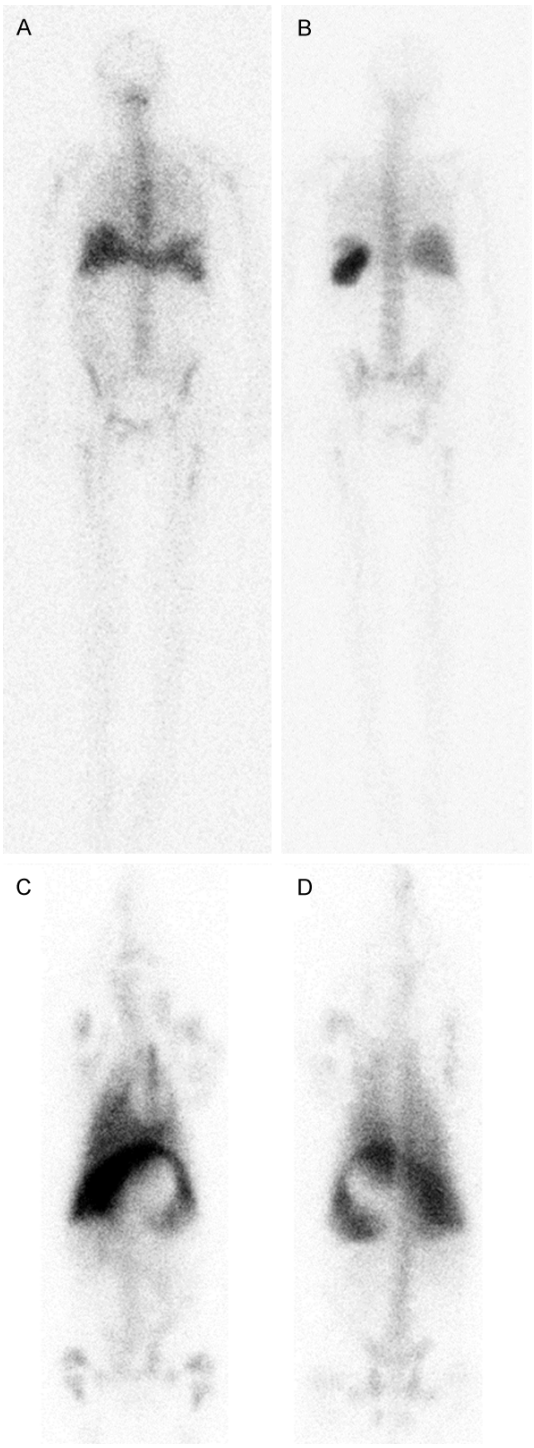

Figure 5. Whole body ^{111}In-leucocyte scintigraphy of adult human 24 h after inoculation in A: Anterior view and B: Posterior view and of a 12-weeks old juvenile pig 6 h after inoculation [19] in C: Ventral and D: Dorsal view. The central sparing in the pig between liver and spleen represents a full stomach. As in humans prolonged clearance of activity from labeled leukocytes from liver and spleen is seen as well as low excretion activity in both feces and urine. The major difference was the accumulation of activity in the lungs of juvenile pigs, which is only a transient phenomenon in healthy human lungs.

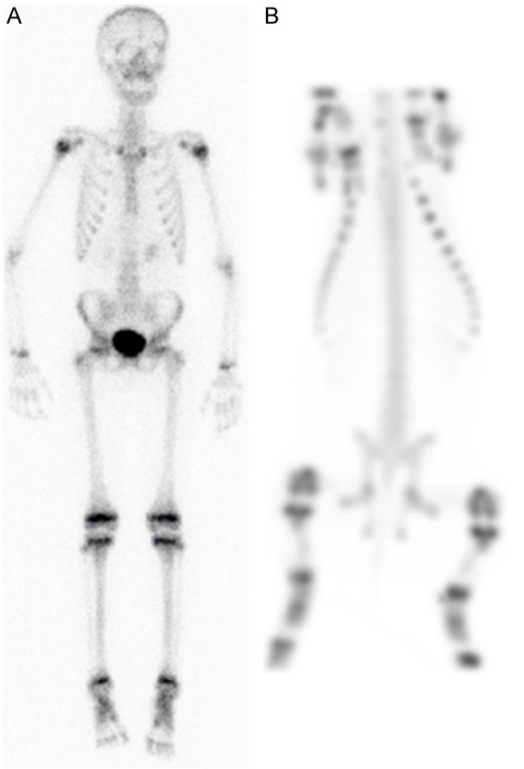

Figure 6. Whole body ^{99m}Tc-DPD bone scintigraphy of A: 7-years old child (anterior view) and B: 12-weeks old pig (ventral view MIP).

Although it is mainly used for oncological imaging, ^{18}F-FDG has also been tested for inflammation imaging. ^{18}F-FDG accumulates in cells that show an increased glucose metabolism. This *non*-specific behavior also allows the ^{18}F-FDG to enter leukocytes present in inflammation. Semi quantitative analysis, which may be useful for differentiating infections from inflammation and monitoring response to therapy, is easily performed with PET, but less feasible with scintigraphy. ^{18}F-FDG PET scan can be performed quicker than leukocyte SPECT: 1 hrs after injection compared to several hrs. In the osteomyelitic model, ^{18}F-FDG performed very well, detecting all osteomyelitic lesions (**Table 3**).

The naturally occurring essential amino acid methionine, in the form of the tracer ^{11}C-methionine, is crucial for protein and phospholipid synthesis and can visualize sites of cell growth and replication after transportation into the cell by the L-type amino acid transporter (LAT) 1 [46]; and thus will accumulate in sites of infection, where both amino acid transport and metabolism take places. Previously, we

were not able to demonstrate ^{11}C-methionine as a reliable marker of ostemyelitis [16, 19], as only 50%, i.e. 2 of 4, of subacute osteomyelitic lesions were identified. By increasing the activity from approximately 8-10 MBq per kg to 18 to 28 MBq per kg in the present study, it was possible to visualize osteomyelitis in 19 of 24 cases (79%) (**Table 3**); and obtain far better lesion to background activity (**Figure 3**), allowing improved interpretation. Methionine had a tendency to accumulate profound in the lesions. Biodistribution of ^{11}C-methionine has been evaluated in children and young adults who were given an activity of 740 MBq of ^{11}C-methionine per 1.7 m^2 of body surface area (maximum prescribed dose, 740 MBq) the age ranged from 2 to 29 y (median 12 y), and PET images were acquired approximately 5-15 min later [47]. In another study 11 MBq was given per kg bodyweight (maximum 740 MBq), age range 2-21 y (mean age 15 y±5 y) [48]. In the latter study tracer accumulation was recorded over 60 min directly after tracer injection or over 40 min beginning 20 min after tracer injection. Summed activity from 20 to 60 min after tracer injection was used for image reconstruction. Only images of the brain were presented. The ^{11}C-activity in our whole body scan presented here was reduced to 1/8 since dynamic scans of the hind limbs (data not shown) were performed for the first hour after the tracer was given, and still the detectability was reasonable.

^{11}C-methoxy-donepezil is a noncompetitive reversible acetylcholinesterase ligand and was previously validated for imaging cerebral levels of acetylcholinesterase [49]. The bio-distribution of ^{11}C-donepezil for imaging acetylcho-linesterase densities in human peripheral organs has been examined recently, and significant ^{11}C-donepezil uptake was also demonstrated in a post-operative abscess of a pig [24]. *Non*-neuronal cholinergic signaling is involved in immune responses to infections, especially lymphocytes [50]. We therefore tested the tracer in our osteomyelitis model. The tracer accumulated in 14 of 24 osteomyelytic lesions (58%) (**Table 3**), indicating no or low cholinesterase activity in some lesions, which may be an effect of cell type. Taking the short half-life of ^{11}C into account only 1/16 to 1/8 of activity may be expected at time of static scan.

The aim is always to apply as low activity for children as possible, The choice of imaging modality must depend on the individual case and the nature of the illness; is it serious and life-threatening, then a rapid diagnosis may be required, and PET/CT may be considered, especially as our study has shown that ^{18}F-FDG PET has a high accuracy, in the case of osteomyelitis. The highest radiation contribution originates as a rule from CT, and low-dose CT may be chosen. We have planned to look further into these details in future experiments.

In conclusion, ^{18}F-FDG was a very good marker of osteomyelitis in the juvenile appendicular pig skeleton as it detected all 24 osteomyelitis lesions. As ^{18}F-FDG PET/CT can be performed within an hour, can detect all osteomyelitic lesions only 7 days after inoculation it may be considered also in children for early diagnosis accelerating treatment initiation and thus sparing other less reliable imaging techniques, which eventually may delay the diagnosis. The late 24 h ^{111}In labeled leukocyte scintigraphy was reasonably good. However, 24 h imaging of ^{111}In-labeled leukocytes did not improve detectability of osteomyelitic lesions compared to 6 h imaging. It thus may be possible to scan within a shorter time schedule. ^{11}C-donepezil could detect osteomyelitis but was not a suitable marker due to its weak accumulation in lesions. This was probably due to the dynamic scans taking place before the static PET/CT delaying the static PET of the lesions. The trophic markers ^{99m}Tc-DPD and ^{11}C-methionine acted in completely different ways. ^{99m}Tc-DPD detected no lesions, whereas methionine detected 79% of lesions and showed superior accumulation in all enlarged, probably reactive, lymph nodes, indicating that methionine is a better marker of probably repair processes in early stage osteomyelitis.

Acknowledgements

This work was supported by grant no. 0602-01911B (11-107077) from the Danish Council for Independent Research, Technology and Production Sciences. The authors are grateful for the technical support provided by Dennis Brok, Betina Gjedsted Andersen, Elisabeth Wairimu Petersen, Malene Hylle, Hanne Thaagaard Larsen, Rikke Skall, Janne Frederiksen, Lotte S. Meyer, Lena Mortensen, Mie Ringga-

ard Dollerup, Dorte Smith, Rikke Bertelsen, Karin M Nielsen, Peter MH Heegaard, and Páll S. Leifsson.

Disclosure of conflict of interest

None.

Address correspondence to: Pia Afzelius, Department of Diagnostic Imaging, North Zealand Hospital, Hillerød, Dyrehavevej 29, 3400-Denmark, University Hospital of Copenhagen, Copenhagen, Denmark. E-mail: pia.afzelius@dadlnet.dk

References

[1] Krogstad P. Osteomyelitis. In: Feigin RD, Cherry JD, Demmler-Harrison GJ, Kaplan SL, eds. Pediatric infectious diseases. 6th ed. Philadelphia: Saunders, 2009: 725-42.

[2] Gafur OA, Copley LA, Hollmig ST, Browne RH, Thornton LA and Crawford SE. The impact of the current epidemiology of pediatric musculoskeletal infection on evaluation and treatment guidelines. J Pediatr Orthop 2008; 28: 777-785.

[3] Riise OR, Kirkhus E, Handeland KS, Flato B, Reiseter T, Cvancarova M, Nakstad B and Wathne KO. Childhood osteomyelitis-incidence and differentiation from other acute onset musculoskeletal features in a population-based study. BMC Pediatr 2008; 8: 45-54.

[4] Jones HW, Beckles VL, Akinola B, Stevenson AJ and Harrison WJ. Chronic haematogenous osteomyelitis in children: an unsolved problem. J Bone Joint Surg Br 2011; 93: 1005-1010.

[5] Mantero E, Carbone M, Calvo MG, Boero S. Diagnosis and treatment of pediatric chronic osteomyelitis in developing countries: Prospective study of 96 patients treated in Kenya. Musculosceletal Surg 2011; 95: 13-8.

[6] Onche II, Obiano SK. Chronic osteomyelitis of long bones: Reasons for delay in presentation. Niger J Med 2004; 13: 355-8.

[7] Museru LM, Mcharo CN. Chronic osteomyelitis: A continuing orthopaedic challenge in developing countries. Int Orthop 2001; 25: 127-31.

[8] Ikpeme IA, Ngim NE, Ikpeme AA. Diagnosis and treatment of pyogenic bone infections. Afr Health Sci 2010; 10: 82-8.

[9] Lauschke FH, Frey CT. Hematogenous osteomyelitis in infants and children in the northwestern region of Namibia. Management and two-year results. J Bone Joint Surg Am 1994; 76: 502-10.

[10] Jones HW, Harrison JW, Bates J, Evans GA, Lubega N. Radiologic classification of chronic hematogenous osteomyelitis in children. J Pediatr Orthop 2009; 29: 822-7.

[11] Yochum TR, Rowe LJ. Essentials of skeletal radiology. Lippincott Williams & Wilkins. (1996) ISBN: 0683093304.

[12] Harris WH, Heaney RP. Skeletal renewal and metabolic bone disease. N Engl J Med 1969; 280: 193-202.

[13] Peltola H and Paakkonen M. Acute osteomyelitis in children. N Engl J Med 2014; 370: 352-360.

[14] Pineda C, Vargas A, RodriGuez AV. Imaging of osteomyelitis; current concepts. Infect Dis Clin North Am 2006; 20: 789-825.

[15] Jamar J, Buscombe J, Chiti A, Christian PE, Delbeke D, Donohoe KJ, Israel O, Martin-Comin J, Signore A. EANM/SNMMI Guideline for 18F-FDG Use in Inflammation and Infection. J Nucl Med 2013; 54: 647-658.

[16] Nielsen OL, Afzelius P, Bender D, Schønheyder HC, Leifsson PS, Nielsen KM, Larsen JO, Jensen SB, Alstrup AK. Comparison of autologous ^{111}In-leukocytes, ^{18}F-FDG, ^{11}C-methionine, ^{11}C-PK11195 and ^{68}Ga-citrate for diagnostic nuclear imaging in a juvenile porcine haematogenous *staphylococcus aureus* osteomyelitis model. Am J Nucl Med Mol Imaging 2015; 5: 169-182.

[17] Das UN. Acetylcholinesterase and butyrylcholinesterase as possible markers of low-grade systemic inflammation. Med Sci Monit 2007; 13: RA214-21.

[18] Johansen LK, Svalastoga EL, Frees D, Aalbaek B, Koch J, Iburg TM, Nielsen OL, Leifsson PS and Jensen HE. A new technique for modeling of hematogenous osteomyelitis in pigs: inoculation into femoral artery. J Invest Surg 2013; 26: 149-153.

[19] Afzelius P, Nielsen OL, Alstrup AKO, Bender D, Leifsson PS, Jensen SB, Schønheyder HC. Biodistribution of the radionuclides ^{18}F-FDG, ^{11}C-methionine, ^{11}C-PK11195, and ^{68}Ga-citrate in domestic juvenile female pigs and morphological and molecular imaging of the tracers in hematogenously disseminated *Staphylococcus aureus* lesions. Am J Nucl Med Mol Imaging 2016; 6: 42-58.

[20] Nielsen OL, Iburg T, Aalbaek B, Leifsson PS, Agerholm JS, Heegaard P, Boye M, Simon S, Jensen KB, Christensen, S, Melsen K, Bak AK, Backman ER, Jørgensen MH, Groegler DK, Jensen AL, Kjelgaard-Hansen M and Jensen HE. A pig model of acute *Staphylococcus aureus* induced pyemia. Acta Vet Scand 2009; 51: 14.

[21] Alstrup AK, Nielsen KM, Schønheyder HC, Jensen SB, Afzelius P, Leifsson PS, Nielsen OL. Refinement of a hematogenous localized osteomyelitis model in pigs. Scandinavian Journal of Laboratory Animal Science 2015; 41: 1-4.

[22] Heegaard PM, Pedersen HG, Jensen AL and Boas U. A robust quantitative solid phase immunoassay for the acute phase protein C-reactive protein (CRP) based on cytidine 5'-diphosphocholine coupled dendrimers. J Immunol Methods 2009; 343: 112-118.
[23] Buus S, Grau C, Munk OL, Bender D, Jensen K, Keiding S. 11C-methionine PET, a novel method for measuring regional salivary gland function after radiotherapy of head and neck cancer. Radiother Oncol 2004; 73: 289-96.
[24] Gjerløff T, Jakobsen S, Nahimi A, Munk OL, Bender D, Alstrup AK, Vase KH, Hansen SB, Brooks DJ, Borghammer P. In vivo imaging of human acetylcholinesterase density in peripheral organs using 11C-donepezil: dosimetry, biodistribution, and kinetic analyses. J Nucl Med 2014; 55: 1818-24.
[25] Comar D, Cartron J, Maziere M and Marazano C. Labelling and metabolism of methionine-methyl-11 C. Eur J Nucl Med 1976; 1: 11-14.
[26] International Commission on Protection. Annals of the IRCP Publication 53, Radiation Dose to Patients from Radiopharmaceuticals. Pergamon, Elsevier Science 1988, pp. 255-6.
[27] Roca M, de Vries EF, Jamar F, Israel O and Signore A. Guidelines for the labeling of leucocytes with (111)In-oxine. Inflammation/Infection Taskgroup of the European Association of Nuclear Medicine. Eur J Nucl Med Mol Imaging 2010; 37: 835-841.
[28] Alstrup AK, Winterdahl M. Imaging techniques in large animals. Scandinavian Journal of Laboratory Animal Science 2009; 36: 1-12.
[29] Jødal L, Afzelius P and Jensen SB. Influence of positron emitters on standard gamma-camera imaging. J Nucl Med Technol 2014; 42: 42-50.
[30] Madsen LW and Jensen HE. In: Jensen HE, editor. Necropsy of the Pig. Necropsy A Handbook and Atlas. Frederiksberg: Biofolia; 2011. pp. 83-106.
[31] Sullivan DC, Rosenfield NS, Ogden J, Gottschalk A. Problems in the scintigraphic detection of osteomyelitis in children. Radiology 1980: 135; 731-736.
[32] Nadel HR. Bone scan update. Semin Nucl Med 2007; 37: 332-339.
[33] Aiger RM, Fueger GF, Ritter G. Results of three-phase bone scintigraphy and radiography in 20 cases of neonatal oseomyelitis. Nucl Med Commun 1996; 17: 20-28.
[34] Johansen LK, Koch J, Kirketerp-Møller K, Wamsler OJ, Nielsen OL, Leifsson PS, Frees D, Aalbæk B, Jensen HE. Therapy of haematogenous osteomyelitis - a comparative study in a porcine model and Angolan children. In Vivo 2013; 27: 305-312.
[35] Johansen LK, Iburg TM, Nielsen OL, Leifsson PS, Dahl-Petersen K, Koch J, Frees D, Aalbæk B, Heegaard PM, Jensen HE. Local osteogenic expression of cyclooxygenase-2 and systemic response in porcine models of osteolyelitis. Prostaglandins Other Lipid Mediat 2012; 97: 103-108.
[36] Zakhireh B, Thakur ML, Malech HL, Cohen MS, Gottschalk A, Root RK. Indium-111-labeled polymorphonuclear leukocytes: viability, random migration, chemotaxis, bactericidal capacity and ultrastructure. J Nucl Med 1979; 20: 741-747.
[37] Thakur M, Segal A, Louis L, Welch MJ, Hopkins J, Peters TJ. Indium-111-labelled cellular blood components: Mechanism of labelling and intracellular location in human neutrophils. J Nucl Med 1977; 18: 1022-1026.
[38] Silvester D, Waters S. Dosimetry of radiolabelled white blood cells. Int J Nucl Biol 1983; 10: 141-144.
[39] Thakur M, McAfee J. The significance of chromosomal aberrations in indium-111-labelled lymphocytes. J Nucl Med 1984; 25: 922-927.
[40] Liberatore M, Iurilli AP, Ponzo F, Prosperi D, Santini C, Baiocchi P, Rizzo L, Speziale F, Fiorani P, Centi Colella A. Clinical usefulness of technetium-99m-HMPAO-labeled leukocyte scan in prosthetic vascular graft infection. J Nucl Med 1998; 39: 875-879.
[41] Larikka MJ, Ahonen AK, Junila JA, Niemela O, Hamalainen MM, Syrjala HP. Extended combined 99mTc-white blood cell and bone imaging improves the diagnostic accuracy in the detection of hip replacement infections. Eur J Nucl Med 2001; 28: 288-293.
[42] Krznaric E, Roo MD, Verbruggen A, Stuyck J, Mortelmans L. Chronic osteomyelitis: diagnosis with technetium-99m-d, l-hexamethylpropylene amine oxime labelled leucocytes. Eur J Nucl Med 1996; 23: 792-797.
[43] Rini JN, Bhargava KK, Tronco GG, Singer C, Caprioli R, Marwin SE, Richardson HL, Nichols KJ, Pugliese PV, Palestro CJ. PET with FDG-labeled leukocytes versus scintigraphy with 111In-oxine-labeled leukocytes for detection of infection. Radiology 2006: 238; 978-87.
[44] The Imaging of Infection and Inflammation. Ed. PH Cox, JR Buscombe. Springer Science and Business Media 2012, pp. 135.
[45] Society of Nucl Med Procedure Guideline for 111In-leucocyte scintigraphy for suspected Infection/Inflammation. Version 3.0, 2004.
[46] Fuchs BC, Bode BP. Amino acid transporters ASCT2 and LAT1 in cancer: partners in crime? Semin Cancer Biol 2005; 15: 254-266.
[47] Haris SM, Davis JC, Snyder SE, Butch ER, Vāvere AL, Kocak M, Shulkin BL. Evaluation of the Biodistribution of ^{11}C-Methionine in Children and Young Adults. J Nucl Med 2013; 54: 1902-1908.

[48] Galldiks N, Kracht LW, Berthold F, Miletic H, Klein JC, Jacobs AH, Heiss WD. [11C]-L-Methionine positron emission tomography in the management of children and young adults with brain tumors. J Neurooncol 2010; 96: 231-239.

[49] Okamura N, Funaki Y, Tashiro M, Kato M, Ishikawa Y, Maruyama M, Ishikawa H, Meguro K, Iwata R, Yanai K. In vivo visualization of donepezil binding in the brain of patients with Alzheimer's disease. Br J Clin Pharmacol 2008; 65: 472-9.

[50] Kawashima K, Fujii T, Moriwaki Y, Misawa H. Critical roles of acetylcholine and the muscarinic and nicotinic acetylcholine receptors in the regulation of immune function. Life Sci 2012; 91: 1027-1032.